The Journal of Chemical Physics ARTICLE pubs.aip.org/aip/jcp

The effects of ionic valency and size asymmetry on counterion adsorption

Cite as: J. Chem. Phys. 164, 224906 (2026); doi: 10.1063/5.0336084
Submitted: 28 March 2026 • Accepted: 20 May 2026 •
Published Online: 12 June 2026

View Online Export Citation CrossMark

Or Ben Yaakov,[1] Haim Diamant,[2] Rudolf Podgornik,[3,4,5,a)] and David Andelman[1,b)]

AFFILIATIONS

[1] School of Physics and Astronomy and Center for Physics and Chemistry of Living Systems, Tel Aviv University, Tel Aviv 6997801, Israel
[2] School of Chemistry and Center for Physics and Chemistry of Living Systems, Tel Aviv University, Tel Aviv 6997801, Israel
[3] School of Physical Sciences and Kavli Institute for Theoretical Sciences, University of Chinese Academy of Sciences, Beijing 100049, China
[4] Wenzhou Institute, University of Chinese Academy of Sciences, Wenzhou, Zhejiang 325000, China
[5] CAS Key Laboratory of Soft Matter Physics, Institute of Physics, Chinese Academy of Sciences, Beijing 100190, China

Note: This paper is part of the Special Topic on Statistical Physics: From Quantum Fluctuations to Soft Matter and Viral Assemblies.
[a)] Deceased, 28 December 2024.
[b)] **Author to whom correspondence should be addressed:** andelman@post.tau.ac.il

ABSTRACT

We study the effect of asymmetry in solvent and ionic size on the equilibrium properties of multivalent ionic solutions near a charged surface. For a single ionic species in solution, we derive a generalized Grahame equation at the charged surface. For a general size ratio between the ions and the solvent, we obtain analytical results for the concentration profiles as a function of the distance from the surface. For a weak surface charge and small ion-to-solvent size ratio, the profile follows the classical Poisson–Boltzmann equation in dilute solution conditions. However, for high surface charge and large ionic size, the concentration profile saturates near the surface, leading to distinctive dependencies of the solution properties on the surface charge density and size asymmetry. Furthermore, the crossover between dilute and saturated regimes depends on the surface charge and ionic size asymmetry. We suggest that a solution containing multiple ionic species of different valencies and sizes stratifies close to the surface in the saturation regime. This leads to the formation of layers that are ordered according to the ions' valency-to-size ratio.

© 2026 Author(s). All article content, except where otherwise noted, is licensed under a Creative Commons Attribution (CC BY) license (https://creativecommons.org/licenses/by/4.0/). https://doi.org/10.1063/5.0336084

12 June 2026 19:36:57

I. INTRODUCTION

Electrostatic interactions between small and macro ions in aqueous solutions govern the self-organization and dynamics of numerous soft matter and biological systems, such as charged colloid suspensions, charged biomembranes, proteins, polyelectrolytes, and DNA. For dilute ionic solutions, the Poisson–Boltzmann (PB) theory[1,2] is rather successful in describing equilibrium solution properties. The main advantage of the PB theory is its simplicity, which allows for analytical or numerical solutions, in broad agreement with experiments.

At higher concentrations (above 1M for monovalent salts, corresponding to an inter-ion distance of about 1.2 nm), steric and other short-range interactions as well as ion–ion correlations become important, and more refined theories are needed. In particular, as the PB theory does not account for the finite ion size, it does not predict a maximal density (saturation) at charged surfaces in cases where the ionic density approaches close packing. These effects require modifications of the PB theory, either in terms of corrections that go beyond mean field, non-electrostatic contributions or using a lattice-gas model that accounts for the mixing entropy more correctly.[2,3]

© Author(s) 2026

One of these extensions is the *sterically modified* PB (sMPB) theory that accounts for the finite ionic and solvent (water) molecular volume via a lattice-gas model for the mixing entropy.[4,5] The conceptual basis of this approximation is to combine the Poisson equation of electrostatics with a lattice-gas entropy of mixing, accounting also for the solvent entropy.

In the more specific case where the ions and solvent (water) molecules have roughly the same size, it is possible to obtain analytical predictions[2,4,5] and a description of the ion concentration saturation close to charged surfaces. The more general case of ions and solvents having different molecular sizes has also been studied in experiments, theory, and numerical simulations.[6–15] For example, ionic solutions containing multiple counterions were shown to exhibit stratification close to a strongly charged surface, where the concentration of different counterion species peaks at different distances from the surface.

In the present study, we incorporate size asymmetry effects using the Flory–Huggins entropy of mixing. We extend the mean-field theory used in Refs. 14 and 15 and present results for the multivalent ion concentration and electrostatic potential profiles close to charged surfaces. One of our main results is to show how the ionic valency-to-size ratio determines the order in which different ionic layers stratify close to the surface.

The outline of this paper is as follows. Section II presents the model applicable to a single counterion species near a charged surface, whose size differs from the solvent's. A modified PB equation is obtained in the dilute and saturated regimes, and the effect of size-asymmetric steric repulsion is presented for strongly charged surfaces. Then, in Sec. III, we generalize the model for a multi-species ionic solution, and the profile equations, the Grahame equation, and the osmotic pressure are derived. We apply our findings from the single-counterion case to propose a theoretical argument for the stratification effect in multi-species ionic solutions. We end up presenting the conclusions and connections with experiments in Sec. IV.

II. MODEL FOR A SINGLE COUNTERION SOLUTION

We derive the free energy of an aqueous ionic solution using a discrete lattice-gas formulation with the ions and solvent molecules fully occupying a three-dimensional cubic lattice. The lattice cell volume, a^3, is taken as the volume of a solvent molecule.

In the first step, we consider a solution containing only a single ionic species (counterion) of molecular volume a^3v and an opposite charge $q = ze < 0$ to the surface charge, where z is the valency and e the electronic charge. The parameter v is the ratio between the molecular volume of the counterion and that of the solvent (a^3).

In the more common case of an electrolyte solution, the validity of such a counterion-only model depends on the inequality of two lengths, $l_{GC} \ll \lambda_D$. The first length, $l_{GC} \sim T/\sigma$, is the Gouy–Chapman length[2] defined in Eq. (15), which depends on the temperature T and the surface charge density σ. The second, $\lambda_D \sim \sqrt{T/n}$, is the Debye screening length[2] that depends on T and the monovalent bulk electrolyte concentration, n. The limit $l_{GC} \ll \lambda_D$ implies that σ should be sufficiently large and/or Tn sufficiently small.

The free energy, $F = U_{el} - TS$, is expressed in terms of the local electrostatic potential $\psi(\boldsymbol{r})$ and the counterion number concentration $c(\boldsymbol{r})$ and volume fraction $\phi(\boldsymbol{r}) = a^3vc(\boldsymbol{r})$. The electrostatic contribution is[2]

$$U_{el} = \int d^3r\left(-\frac{\varepsilon}{2}|\nabla\psi|^2 + qc\psi\right). \tag{1}$$

The first term is the electric field's self-energy, where ε is the dielectric constant; the second term is the sum of the ions' electrostatic energy. The Flory–Huggins entropic contribution to the free energy is written as

$$-TS = \frac{k_BT}{a^3}\int d^3r\left(\frac{\phi}{v}\ln\phi + (1-\phi)\ln(1-\phi)\right), \tag{2}$$

where k_BT is the thermal energy. The first term is the counterions' mixing entropy. The second one is the mixing entropy of the solvent whose volume fraction is $1-\phi$.

At equilibrium, the system has a spatially uniform thermodynamic pressure P, which can be derived, e.g., through the contact theorem.[16,17] It yields the following equation of state:

$$-\frac{Pa^3}{k_BT} = \frac{a^3\varepsilon}{2k_BT}|\nabla\psi|^2 + \ln(1-\phi) + w\phi = \text{const}, \tag{3}$$

where we make use of another size parameter, $w \equiv 1 - 1/v$. The first term on the right-hand-side of Eq. (3) is the contribution to the pressure from the electrostatic stress, while the second and third terms come from the lattice-gas entropy pressure. At equilibrium, the total pressure is uniform. It can be evaluated at a reference position, where the electrostatic field vanishes. This determines the constant of Eq. (3).

A. Counterion profile equations

Minimizing the total free energy with respect to ψ yields the Poisson equation, expressed in terms of volume fraction,

$$\nabla^2\psi = -\frac{1}{\varepsilon}\frac{q\phi(\boldsymbol{r})}{a^3v}. \tag{4}$$

Next, minimizing the free energy with respect to c (or ϕ) gives the equation of state for the ionic concentration,

$$\frac{\phi}{(1-\phi)^v} = \frac{\phi_{ref}}{(1-\phi_{ref})^v}e^{-\beta q\psi}, \tag{5}$$

where $\beta = 1/k_BT$ is the inverse thermal energy and ϕ_{ref} and $1-\phi_{ref}$ are, respectively, the counterion and solvent volume fractions at the reference position, where $\psi_{ref} = 0$. Equation (5) for general v is a transcendental equation with no analytical solution for ϕ. Together with Eq. (3), these two equations can be solved with the proper boundary conditions in order to obtain the density profile $\phi(\boldsymbol{r})$ and local potential $\psi(\boldsymbol{r})$.

We can now derive the profile equations in the dilute ($\phi \ll 1$) and saturation ($1-\phi \ll 1$) limits. In the following, we define η as the solvent local fraction,

$$\eta(\boldsymbol{r}) \equiv 1 - \phi(\boldsymbol{r}). \tag{6}$$

For the dilute limit, neglecting the solvent contribution in Eq. (5), we recover the standard Boltzmann distribution,

$$\phi(\boldsymbol{r}) \approx \phi_{ref}e^{-\beta q\psi(\boldsymbol{r})}. \tag{7}$$

12 June 2026 19:36:57

© Author(s) 2026

On the other hand, at the saturation limit, the solvent volume fraction η is the small parameter. We rewrite Eq. (5) as

$$\frac{\eta(\boldsymbol{r})}{[1-\eta(\boldsymbol{r})]^{1/v}} = \mathrm{e}^{-\beta[\mu - q\psi(\boldsymbol{r})]/v}, \qquad \beta\mu = \ln\phi_{\mathrm{ref}} - v\,\ln(1-\phi_{\mathrm{ref}}). \tag{8}$$

Expanding to the first order in η, we find that the solvent volume fraction follows a modified Boltzmann distribution

$$\eta(\boldsymbol{r}) \approx \mathrm{e}^{-\beta[\mu - q\psi(\boldsymbol{r})]/v}, \tag{9}$$

while the counterion volume fraction approaches saturation with an exponentially small correction term that depends on the electrostatic potential,

$$\phi(\boldsymbol{r}) \approx 1 - \mathrm{e}^{-\beta[\mu - q\psi(\boldsymbol{r})]/v}. \tag{10}$$

Compared to Eq. (7) of the dilute limit, Eqs. (8)–(10) of the saturation limit contain an extra factor of $1/v$ in the exponent. A simple argument can explain the origin of this size dependency. Consider that the ions in the saturated regime ($\phi \lesssim 1$) are in a system of volume V. Then, slightly dilute the system by adding a small amount of solvent, such that $\eta \to \eta + \delta\eta$. As all lattice cells are occupied, the ionic volume fraction changes by $\delta\phi = -\delta\eta$, and each solvent molecule replaces $1/v$ ions. The resulting change in free energy has three contributions,

$$\begin{aligned} &\left(\frac{V}{a^3}\right) k_{\mathrm{B}}T(\ln\eta - 1)\,\delta\eta && \text{mixing entropy gain,}\\ &\left(\frac{V}{va^3}\right) q\psi\,\delta\phi = -\left(\frac{V}{va^3}\right) q\psi\,\delta\eta && \text{electrostatic penalty,}\\ &\left(\frac{V}{va^3}\right)\mu\,\delta\phi = -\left(\frac{V}{va^3}\right)\mu\,\delta\eta && \text{chemical potential.} \end{aligned} \tag{11}$$

Minimizing the total change in free energy with respect to $\delta\eta$, we obtain $\delta\eta = \exp[-\beta(\mu - q\psi)/v]$, in agreement with Eq. (9).

B. Counterion adsorption on a charged surface

We now explore the ionic profile for the single counterion species near a charged surface with charge density $\sigma > 0$. We assume that the system is homogeneous in the directions parallel to the surface. The profiles are then only a function of the distance away from the surface, x, making the system one-dimensional (1D). As the pressure is uniform, it can be evaluated [Eq. (3)] at infinite distance from the surface, where the electrostatic field vanishes $\psi'(x \to \infty) = 0$. The counterions have to balance the surface charge, and their concentration vanishes at infinity, $\phi(x \to \infty) = 0$ and $\eta(\infty) = 1$. Hence, the pressure in this counterion-only case is zero, and Eq. (3) can be rearranged as

$$\ln\eta + w\phi = -\frac{a^3\varepsilon}{2k_{\mathrm{B}}T}|\nabla\psi|^2. \tag{12}$$

1. The generalized Grahame equation

Substituting the electrostatic boundary condition, $\psi'(x=0) = -\sigma/\varepsilon$ in Eq. (3), we obtain the condition for the counterion fraction at the surface, $\phi_{\mathrm{s}} \equiv \phi(0)$, expressed via a dimensionless surface parameter ζ,

$$\ln(1-\phi_{\mathrm{s}}) + w\phi_{\mathrm{s}} = -\zeta. \tag{13}$$

This is a modification of the Grahame equation[2] where

$$\zeta = 2\pi l_{\mathrm{B}} a^3 \left(\frac{\sigma}{e}\right)^2 = \frac{a^3}{2\pi l_{\mathrm{B}} l_{\mathrm{GC}}^2}, \tag{14}$$

and the Bjerrum length l_{B} and Gouy–Chapman length l_{GC} are defined[2] as usual,

$$l_{\mathrm{B}} = \frac{e^2}{\varepsilon k_{\mathrm{B}}T}, \quad l_{\mathrm{GC}} = \frac{1}{2\pi l_{\mathrm{B}}}\frac{e}{\sigma}. \tag{15}$$

Throughout the paper, we take the relative dielectric constant of water to be 80. At room temperature, $T = 300$ K, this leads to $l_{\mathrm{B}} \simeq 7$ Å. Since the dimensionless surface parameter ζ does not depend on v, the effect of the ion size on ϕ_{s} enters only through the parameter $w = 1 - 1/v$ defined earlier.

The solution to the transcendental Eq. (13) can be expressed in terms of the Lambert W function (also called the *product logarithm*), $W(u)$, defined as the inverse function of $u(W) = W\mathrm{e}^W$,

$$\phi_{\mathrm{s}} = 1 + \frac{1}{w} W\left(-w\mathrm{e}^{-\zeta - w}\right). \tag{16}$$

Equation (16) is one of our central results. It can be viewed as a generalized Grahame equation, relating the counterion fraction at the surface, $\phi(0) = \phi_{\mathrm{s}}$, with the surface charge density σ for a single counterion species of arbitrary size asymmetry.

Equation (16) is presented in Fig. 1 for both a weakly charged surface ($\zeta = 0.5$) and a strongly charged one ($\zeta = 2$). [Note that even for small (but not vanishing) values of ζ, the counter-ion-only model can be justified for dilute enough electrolytes. Moreover, $\zeta \sim a^3$, where a is the smallest length in the system, implying that ζ can be quite small without affecting the validity of our counter-ion-only model.]

In addition, we present three limiting cases. First, substituting $v = 1$ ($w = 0$, no asymmetry) reproduces the corresponding Grahame equation for the symmetric MPB case,[2]

$$\phi_{\mathrm{s}} = 1 - \mathrm{e}^{-\zeta}. \tag{17}$$

The second limit corresponds to saturation of the ionic concentration near the surface. It can be treated by assuming a large surface charge density σ so that ζ is sufficiently large, and the argument of W is exponentially small. Then, we can expand $W(u)$ to first order in u, $W(u \ll 1) \approx u$, yielding

$$\phi_{\mathrm{s}} \approx 1 - \mathrm{e}^{-\zeta - w}. \tag{18}$$

The argument of W in Eq. (16) depends not only on ζ, but also on v (through $w = 1 - 1/v$). The third limit is that of small ionic size v. Even for large ζ, if the ionic size is sufficiently small such that $v \lesssim v^* = 1/(1+\zeta)$, we cannot use the expansion of W for small arguments. Instead, we should use the asymptotic expansion for large arguments, $W(u \gg 1) \sim \ln u$. This is the case in the limit

12 June 2026 19:36:57

© Author(s) 2026

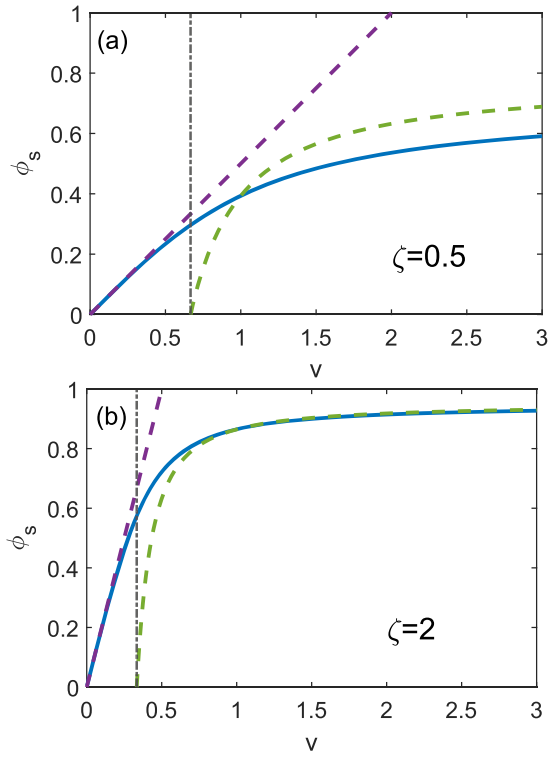

FIG. 1. Counterion fraction at the charged surface ϕ_s (solid blue line) as a function of the size ratio v [Eq. (16)]. (a) The weakly charged surface case; and (b) the strongly charged surface case. Convergence to the low v limit (dashed purple line), Eq. (19), is seen in both cases, whereas in the high v limit (dashed green line), Eq. (18) is a good approximation only for strongly charged surfaces where ϕ_s is close to saturation. The vertical dashed–dotted black line marks the crossover between the two limiting behaviors, $v^* = 1/(1+\zeta)$.

of point-like ions ($v \to 0$), holding for a dilute solution. Then, we recover the Grahame equation of the PB model,[2]

$$c_s \approx 2\pi l_B \left(\frac{\sigma}{e}\right)^2, \quad \phi_s = a^3 v c_s. \tag{19}$$

Therefore, ϕ_s in this limit is proportional to v.

In Fig. 1, we plot ϕ_s as a function of the size asymmetry v for small ζ [$\zeta = 0.5$ in Fig. 1(a)] and large ζ [$\zeta = 2$ in Fig. 1(b)]. The solid blue line represents the full solution from Eq. (16). For large ζ in Fig. 1(b), the approximate Eq. (18) (dashed green line) converges well to the full solution in the limit of large v, reaching the maximum value of $1 - e^{-\zeta-1}$. However, the approximation substantially deviates from the full solution for small ζ [dashed green line in Fig. 1(a)]. The crossover asymmetry $v^* = 1/(1+\zeta)$ is marked by a vertical dashed–dotted line. For $v < v^*$, the solution for ϕ_s tends to the linear curve v, given by the Grahame equation, Eq. (19) (dashed purple line). This is clearly evident for both values of $\zeta < 1$ and $\zeta > 1$ shown in the figure.

2. Ionic profile: $\phi(x)$

Taking the spatial derivative of Eq. (3) and combining it with the Poisson equation [Eq. (4)], we obtain a first-order differential equation relating $\phi(x)$ and its derivative $\phi'(x)$. This equation can be integrated, yielding

$$x(\phi) = \frac{1}{\alpha}\sqrt{\frac{a^3}{8\pi l_B}} \int_{\phi_s}^{\phi(x)} d\phi \, \frac{(1-\phi)^{-1} - w}{\phi\sqrt{-\ln(1-\phi) - w\phi}}, \tag{20}$$

where $\alpha = |z|/v$ is the valency-to-size ratio. Once the boundary value ϕ_s is obtained from Eq. (16), we can calculate the profile $\phi(x)$ numerically by inverting $x(\phi)$ from Eq. (20). Then, using Eq. (5) with $\phi_{ref} = \phi_s$, the profile of the electrostatic potential $\psi(x)$ can be obtained as well.

In a saturated region, the right-hand-side of Eq. (4) tends to a constant, $\psi'' \approx -q/(\varepsilon v a^3)$, and this second-order ODE for 1D symmetry can be integrated twice. The resulting spatial dependence of the electrostatic potential is parabolic,[4]

$$\beta e\psi(x) \approx -\frac{\zeta}{\alpha} + \frac{2\pi l_B \alpha}{a^3}\left(x - \ell^*\right)^2, \qquad \ell^* = a^3\sigma/\alpha e, \tag{21}$$

where the potential at the surface is set as the reference potential, $\psi_{ref} = \psi(x=0) = 0$. Clearly, there is an extremum at a distance ℓ^* from the surface. Since the counterion concentration profile depends exponentially on ψ, Eq. (10), the length ℓ^* characterizes well the thickness of the saturation layer.

Figure 2(a) shows the counterion volume fraction profile, $\phi(x)$, as a function of the distance from the surface, x, obtained from Eq. (20). Similarly, Fig. 2(b) shows the respective electrostatic potential profile, obtained from Eq. (8). The profiles shown are for the symmetric case ($v = 1$; green line), as well as for a smaller size ratio between counterion and solvent ($v = 1/8$; purple line) and a larger one ($v = 8$; blue line). The solvent size a is adjusted while the counterion size va^3 is kept constant. Since $a^3/\alpha \sim va^3$, the characteristic length ℓ^* is also unchanged.

Figure 2 demonstrates the enhanced saturation effect caused by larger solvent molecules. This is due to the smaller entropy gained by mixing the counterions with the larger solvent molecules. From a more intuitive perspective, the large solvent molecules osmotically push the smaller ions closer to the surface.

The volume fraction profiles intersect around $x \approx \ell^*$, demonstrating the role of ℓ^* as a characteristic thickness of the saturated layer. For $x > \ell^*$, the parabolic approximation of the potential profile [Eq. (21)] is no longer valid and deviates largely from the exact profile. Clearly, this approximation can be used only for $x < \ell^*$.

The length ℓ^* can be heuristically inferred from the typical thickness of a saturated layer required to neutralize the charged surface, as follows. The area per surface charge is e/σ. A single counterion of valency z participating in the saturated layer has volume $a^3 v$ and neutralizes $|z|$ monovalent surface charges, i.e., an area of $|z|e/\sigma$. Placing the counterion inside a fictitious rectangular box of base area $|z|e/\sigma$ and volume $a^3 v$ leads to a box length of $va^3\sigma/|z|e$, which is exactly ℓ^* as derived in Eq. (21).

III. FREE-ENERGY AND PROFILES FOR A MULTI-SPECIES IONIC SOLUTION

We now consider the generalization of the single ionic species presented in Sec. II to the case of M ionic species. Each species

12 June 2026 19:36:57

© Author(s) 2026

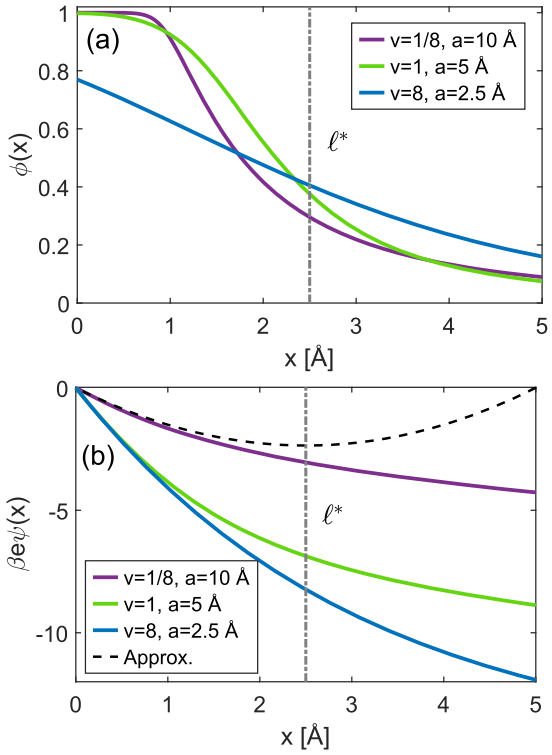

FIG. 2. (a) Counterion volume fraction $\phi(x) = a^3 v c(x)$ and (b) dimensionless electrostatic potential $\beta e\psi(x)$, as a function of distance from the surface, x, for different solvent sizes and size asymmetries. In all cases, the ionic size is held constant, $a^3 v = 125$ Å^3, the ions are monovalent, $z = 1$, and $\alpha = |z|/v = 1/v$. The surface charge density is $\sigma = 2e/\text{nm}^2$. The profiles shown are for the symmetric case ($v = 1, a = 5$ Å, $\zeta \approx 2.7$; green line), as well as for a smaller size ratio between counterion and solvent ($v = 1/8, a = 2.5$ Å, $\zeta \approx 0.3$; purple line) and a larger one ($v = 8, a = 10$ Å, $\zeta \approx 17.6$; blue line). The dashed–dotted vertical line marks the value of $\ell^* = a^3\sigma/\alpha e = 2.5$ Å. Since $a^3/\alpha \sim v a^3$, the characteristic length ℓ^* is unchanged. The approximate parabolic profile of the electrostatic potential (dashed black line) for $v = 1/8$ and $a = 10$ Å is drawn in (b) from Eq. (21).

$i = 1, \ldots, M$, is characterized by a molecular volume $a^3 v_i$ and ionic charge $q_i = z_i e$ (valency z_i). The parameter v_i is the ratio between the molecular volume of the ith ionic species and that of the solvent (a^3).

As in Sec. II, the free energy, $F = U_{\text{el}} - TS$, is expressed in terms of the local electrostatic potential $\psi(\boldsymbol{r})$ and the ionic concentrations $c_i(\boldsymbol{r})$ or, equivalently, volume fractions $\phi_i(\boldsymbol{r}) = a^3 v_i c_i(\boldsymbol{r})$. The electrostatic energy is

$$U_{\text{el}} = \int \mathrm{d}^3 r \left(-\frac{\varepsilon}{2} |\nabla\psi|^2 + \sum_{i=1}^{M} q_i c_i \psi \right). \tag{22}$$

The first term is the electric field's self-energy, and the second term is the sum of the ions' electrostatic energy. Then, the Flory–Huggins entropic contribution to the free energy is written as

$$-TS = \frac{k_B T}{a^3} \int \mathrm{d}^3 r \left(\sum_{i=1}^{M} \frac{\phi_i}{v_i} \ln \phi_i + \eta \ln \eta \right). \tag{23}$$

The first term is the mixing entropy of the ions summed over all ionic species. The second one is the mixing entropy of the solvent. Assuming incompressibility, the solvent local volume fraction is

$$\eta(\boldsymbol{r}) = 1 - \sum_{i=1}^{M} \phi_i(\boldsymbol{r}). \tag{24}$$

At equilibrium, the system has a spatially uniform thermodynamic pressure, which can be derived through the contact theorem.[16,17] It yields the following equation of state that is a generalization of Eq. (3),

$$-\frac{P a^3}{k_B T} = \frac{a^3 \varepsilon}{2 k_B T} |\nabla\psi|^2 + \ln \eta + \sum_{j=1}^{M} w_j \phi_j = \text{const.}, \tag{25}$$

where the parameter w_j is defined as

$$w_j \equiv 1 - 1/v_j. \tag{26}$$

The first term on the right-hand-side of Eq. (25) is the contribution to the pressure from the electrostatic stress, while the second and third terms come from the lattice-gas entropy.

A. Profile equations for *M* ionic species

Minimizing the total free energy with respect to ψ and $\{c_i\}$ (or $\{\phi_i\}$), $i = 1, \ldots, M$, yields the Poisson equation, expressed in terms of volume fractions

$$\nabla^2 \psi = -\frac{1}{\varepsilon} \sum_{i=1}^{M} \frac{q_i \phi_i(\boldsymbol{r})}{a^3 v_i}, \tag{27}$$

and the equation of state for the ionic concentrations,

$$\frac{\phi_i}{\left(1 - \sum_{i=1}^{M} \phi_i\right)^{v_i}} = \frac{\phi_i^{\text{ref}}}{(\eta_{\text{ref}})^{v_i}} \mathrm{e}^{-\beta q_i \psi}, \tag{28}$$

where ϕ_i^{ref} and η_{ref} are, respectively, the volume fractions of the ith species and the solvent at the reference position, where $\psi_{\text{ref}} = 0$.

Equation (28) represents M algebraic equations, containing a polynomial of degree v_i. Together with Eq. (25), we have $M + 1$ equations for the M density profiles $\phi_i(\boldsymbol{r})$ and for the local electrostatic potential $\psi(\boldsymbol{r})$.

B. Stratification of multi-counterion adsorption

Consider a solution containing several counterion species of different size and valency. Close to a strongly charged surface, some experiments[10,11] and numerical studies[6–8] have found that the concentration of lower-valency counterions is higher near the surface. In general, charged surfaces preferentially adsorb high-valency counterions. However, if the lower-valency ions are smaller, this preference can be reversed. Moreover, the above-mentioned studies suggest that the valency-to-size ratio, $\alpha = |z|/v$, determines the spatial order of adsorption (stratification) from a multi-counterion solution—the larger the value of α, the closer the maximal concentration of the ion species to the charged surface. The dependence on α is already seen, indeed, in the expressions for the electrostatic potential ψ and characteristic length ℓ^* of the saturated region, Eq. (21). We now give a semi-quantitative argument to account for these observations.

12 June 2026 19:36:57

© Author(s) 2026

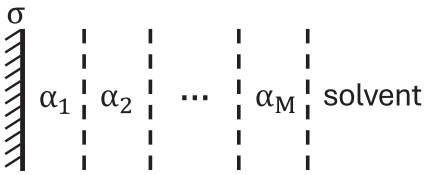

FIG. 3. Schematic of a stratified counterion system near a charged surface. The label α_k represents the dominating species in layer k away from the charged surface. In addition, the stratified layers are characterized by $\alpha_1 > \alpha_2 > \cdots > \alpha_M$.

The solution has M negative ion species with valencies z_i and relative specific volumes v_i (with respect to the solvent molecular size a^3), near a positively charged surface. We assume that the surface is strongly charged, forming a saturated layer of adsorbed counterions, as depicted in Fig. 3. The saturation implies that the electrostatic energy dominates the free energy of adsorption, and mixing entropy can be neglected. Let us further assume that the counterion species are stratified into layers indexed by k according to their distance from the surface. We examine the energy cost of exchanging n_k ions of layer k with n_{k+1} ions of layer $k+1$. For the exchange to be energetically unfavorable, we will prove that the condition has to be $\alpha_{k+1} < \alpha_k$.

Taking the electrostatic potential in the two layers to be ψ_k and ψ_{k+1}, the electrostatic energy cost of the exchange is

$$\begin{aligned}\frac{1}{e}\Delta U_{\rm el} &= \psi_k(n_{k+1}z_{k+1} - n_k z_k) \\ &\quad + \psi_{k+1}(n_k z_k - n_{k+1}z_{k+1}) \\ &= (\psi_k - \psi_{k+1})(n_{k+1}z_{k+1} - n_k z_k) \\ &= -|\psi_k - \psi_{k+1}|(n_{k+1}|z_{k+1}| - n_k|z_k|).\end{aligned} \tag{29}$$

Now, to maintain the condition of saturation in the kth layer,

$$n_{k+1}v_{k+1} - n_k v_k = 0 \quad \Rightarrow \quad n_k/n_{k+1} = v_{k+1}/v_k. \tag{30}$$

Substituting this equation in Eq. (29) yields

$$\frac{1}{e}\Delta U_{\rm el} = |\psi_k - \psi_{k+1}|n_{k+1}v_{k+1}(\alpha_k - \alpha_{k+1}), \tag{31}$$

where we recall that $\alpha_i = |z_i|/v_i$. Therefore, the condition for having $\Delta U_{\rm el} > 0$ (unfavorable exchange) is $\alpha_{k+1} < \alpha_k$. This argument is quite general, provided the electrostatic potential is sufficiently large. Therefore, with increasing distance from the surface, the layers are arranged in decreasing order of the valency-to-size ratio α.

IV. CONCLUSIONS

We have studied the effects of the size asymmetry of ions and solvent on the ionic concentration profiles in an electrolyte solution in contact with a charged surface. We have obtained analytical results for the ionic volume fraction adjacent to the surface, Eq. (16), and (up to an integration) for the full concentration profiles, Eq. (20).

The main findings are summarized in the diagram presented in Fig. 4. The behavior can be separated into three qualitative regimes. In the dilute regime, the PB theory predictions are valid. This

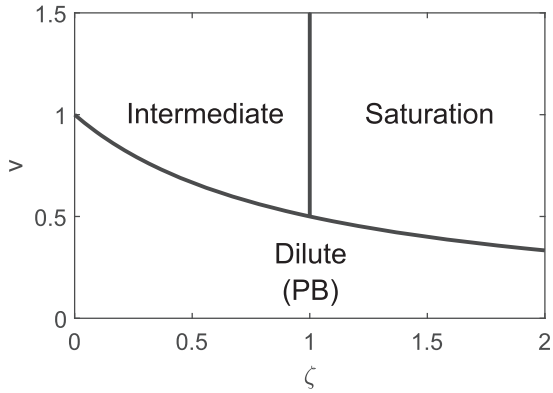

FIG. 4. Three regimes of counterion concentration profiles, plotted on the plane of surface charge ($\zeta \sim \sigma^2$) and size asymmetry (v). The crossover between the intermediate and saturation regimes occurs at $\zeta = 1$, and the one between the dilute and the two other regimes at $v^* = 1/(1+\zeta)$.

regime can be reached by either decreasing the surface charge (σ) or decreasing the ion size relative to the solvent (the v parameter). We have been concerned mainly with the opposite case, of a solution whose concentration profile near the surface is saturated. The saturation regime is reached by a high surface charge σ and a large ion size v relative to the solvent. In this case, the layer structure near the surface has distinctive dependencies on surface charge and size asymmetry, as given by Eq. (18).

The line $v^* = 1/(1+\zeta)$ marks the crossover between the PB regime and two regimes where the PB predictions are not valid anymore. For a weakly charged surface and large ion size ($\zeta < 1$ and $v > v^*$), this intermediate regime is neither well described by the PB theory nor does it have a saturated layer. The saturation regime occurs for $v > v^*$ and $\zeta > 1$.

In addition, our model accounts for stratification in solutions containing multiple counterion species. In this case, separate saturation layers form near the charged surface. The model predicts that stratified layers are ordered according to the valency-to-size ratio of the counterions, $\alpha = |z|/v$, in agreement with earlier observations.[10,11]

Consideration of co-ion species is straightforward by applying the model presented in Sec. III, as performed previously by Maggs and Podgornik.[14] For strongly charged surfaces, co-ions are depleted from the counterion-saturated layer by both the electrostatic repulsion and the steric hindrance. Therefore, we expect our results for the saturation limit to remain unaffected by the inclusion of co-ions.

Since we aim in this study to explore the ionic size effects, we have not considered additional contributions such as specific ion-surface or ion–ion interactions and polar effects. Furthermore, the assumption of a uniform dielectric constant being equal to the solvent's ε is problematic in situations of counterion saturation. In these cases, the solvent molecules are depleted from the region near the surface, or their orientation is strongly affected by the ions.[18,19] This implies that the present treatment overestimates the screening by the aqueous solvent and underestimates the electrostatic interactions. This observation is supported by several models that investigated the combined effects of medium polarizability and ionic finite size.[20–23]

12 June 2026 19:36:57

© Author(s) 2026

The present study can be extended in several directions. Curved geometries (e.g., a charged cylindrical surface or charged sphere) introduce another length scale whose interplay with the ion size should be more complex to analyze and may affect, for example, the Manning–Oosawa condensation[24–26] for the cylindrical case or the effective surface charge for the charged sphere. Another interesting direction is to consider a continuous distribution of ion size and its effects on the concentration and charge density profiles of counterions near charged surfaces.

ACKNOWLEDGMENTS

This article is dedicated to the memory of our dear friend and colleague, Rudolf (Rudi) Podgornik, who participated in the early stages of this work. Rudi made seminal contributions to the field of soft matter physics, and his insight and creativity left a lasting impact on the scientific community. His legacy will continue to inspire colleagues and friends for years to come. D.A. acknowledges partial support from the NSFC-ISF Research Program, jointly funded by the National Science Foundation of China (NSFC) and the Israel Science Foundation (ISF) under Grant No. 3396/19 and ISF Grant No. 226/24. H.D. acknowledges partial support from the NSFC-ISF (Grant No. 3159/23) and the ISF (Grant No. 1611/24).

AUTHOR DECLARATIONS

Conflict of Interest

The authors have no conflicts to disclose.

Author Contributions

Or Ben Yaakov: Conceptualization (equal); Formal analysis (equal); Investigation (equal); Methodology (equal); Software (equal); Visualization (equal); Writing – original draft (equal); Writing – review & editing (equal). **Haim Diamant**: Conceptualization (equal); Formal analysis (equal); Funding acquisition (equal); Investigation (equal); Methodology (equal); Project administration (equal); Supervision (equal); Writing – original draft (equal); Writing – review & editing (equal). **Rudolf Podgornik**: Conceptualization (equal); Methodology (equal). **David Andelman**: Conceptualization (equal); Formal analysis (equal); Funding acquisition (equal); Investigation (equal); Methodology (equal); Project administration (equal); Software (equal); Supervision (equal); Visualization (equal); Writing – original draft (equal); Writing – review & editing (equal).

DATA AVAILABILITY

The data that support the findings of this study are available within the article.

REFERENCES

[1]D. Andelman, in *Handbook of Physics of Biological Systems*, edited by R. Lipowsky and E. Sackmann (Elsevier Science, Amsterdam, 1995), Chap. 12, Vol. I.

[2]T. Markovich, D. Andelman, and R. Podgornik, "Charged membranes: Poisson–Boltzmann theory, DLVO paradigm and beyond," in *Handbook of Lipid Membranes*, edited by C. Safynia and J. Raedler (Taylor & Francis, 2018).

[3]R. Blossey, A. C. Maggs, and R. Podgornik, "Structural interactions in ionic liquids linked to higher-order Poisson–Boltzmann equations," Phys. Rev. E **95**, 060602 (2017).

[4]I. Borukhov, D. Andelman, and H. Orland, "Steric Effects in Electrolytes: A modified Poisson–Boltzmann equation," Phys. Rev. Lett. **79**, 435 (1997).

[5]I. Borukhov, D. Andelman, and H. Orland, "Adsorption of large ions from an electrolyte solution: A modified Poisson–Boltzmann equation," Electrochim. Acta **46**, 221 (2000).

[6]J. Wen, S. Zhou, Z. Xu, and B. Li, "Competitive adsorption and ordered packing of counterions near highly charged surfaces: From mean-field theory to Monte Carlo simulations," Phys. Rev. E **85**, 041406 (2012).

[7]S. Zhou, Z. Wang, and B. Li, "Mean-field description of ionic size effects with nonuniform ionic sizes: A numerical approach," Phys. Rev. E **84**, 021901 (2011).

[8]B. Li, P. Liu, Z. Xu, and S. Zhou, "Ionic size effects: Generalized Boltzmann distributions, counterion stratification and modified Debye length," Nonlinearity **26**, 2899 (2013).

[9]A. Gupta and H. A. Stone, "Electrical double layers: Effects of asymmetry in electrolyte valence on steric effects, dielectric decrement and ion-ion correlations," Langmuir **34**, 11971 (2018).

[10]E. Avraham, B. Yaniv, A. Soffer, and D. Aurbach, "Developing ion electroadsorption stereoselectivity, by pore size adjustment with chemical vapor deposition onto active carbon fiber electrodes. Case of Ca^{2+}/Na^{+} separation in water capacitive desalination," J. Phys. Chem. C **112**, 7385 (2008).

[11]M. E. Suss, "Size-based ion selectivity of micropore electric double layers in capacitive deionization electrodes," J. Electrochem. Soc. **164**, E270 (2017).

[12]Y. Han, S. Huang, and T. Yan, "A mean-field theory on the differential capacitance of asymmetric ionic liquid electrolytes," J. Phys.: Condens. Matter **26**, 284103 (2014).

[13]Y. Zhang and J. Huang, "Treatment of ion-size asymmetry in lattice-gas models for electrical double layer," J. Phys. Chem. C **122**, 28652 (2018).

[14]A. C. Maggs and R. Podgornik, "General theory of asymmetric steric interactions in electrostatic double layers," Soft Matter **12**, 1219 (2016).

[15]K. Sunita, D. Shikha, and R. Podgornik, "On the nature of screening in Voorn–Overbeek type theories," J. Chem. Phys. **156**, 244901 (2022).

[16]M. F. Holovko and J. P. Badiali, "The contact theorem and sum rules in the theory of electrical double layer," Condens. Matter Phys. **8**, 281 (2005).

[17]D. Ben-Yaakov, D. Andelman, D. Harries, and R. Podgornik, "Beyond standard Poisson–Boltzmann theory: Ion-specific interactions in aqueous solutions," J. Phys. Chem. B **113**, 6001 (2009), See the Appendix.

[18]A. Levy, D. Andelman, and H. Orland, "Dipolar Poisson–Boltzmann approach to ionic solutions: A mean field and loop expansion analysis," J. Chem. Phys. **139**, 164909 (2013).

[19]A. Iglič, E. Gongadze, and K. Bohinc, "Excluded volume effect and orientational ordering near a charged surface in solution of ions and Langevin dipoles," Bioelectrochemistry **79**, 223 (2010).

[20]E. Gongadze and A. Iglič, "Decrease of permittivity of an electrolyte solution near a charged surface due to saturation and excluded volume effects," Bioelectrochemistry **87**, 199 (2012).

[21]J. J. Lopez-García and J. Horno, "Poisson-Boltzmann description of the electrical double layer including ion size effects," Langmuir **27**, 13970 (2011).

[22]Y. Nakayama and D. Andelman, "Differential capacitance of the electric double layer: The interplay between ion finite size and dielectric decrement," J. Chem. Phys. **142**, 044706 (2015).

[23]R. M. Adar, T. Markovich, A. Levy, H. Orland, and D. Andelman, "Dielectric constant of ionic solutions: Combined effects of correlations and excluded volume," J. Chem. Phys. **149**, 054504 (2018).

[24]G. S. Manning, "Limiting laws and counterion condensation in polyelectrolyte solutions I. Colligative properties," J. Chem. Phys. **51**, 924 (1969).

[25]F. Oosawa, *Polyelectrolytes* (Marcel Dekker, New York, 1971).

[26]B. O'Shaughnessy and Q. Yang, "Manning–Oosawa counterion condensation," Phy. Rev. Lett. **94**, 048302 (2005).

12 June 2026 19:36:57

© Author(s) 2026